pulmonary nodules using fluorine-18-FDG and PET. *J Nucl Med.* 1996;37:943-8.
24. Imdahl A, Jenkner S, Brink I, et al. Validation of FDG positron emission tomography for differentiation of unknown pulmonary lesions. *Eur J Cardiothorac Surg.* 2001;20:324-9.
25. Lowe VJ, Fletcher JW, Gobar L, et al. Prospective investigation of positron emission tomography in lung nodules. *J Clin Oncol.* 1998; 16:1075-84.
26. Wahl RL, Cody RL, Hutchins GD, et al. Primary and metastatic breast carcinoma: initial clinical evaluation with PET with the radiolabeled glucose analogue 2-[F-18]-fluoro-2-deoxy-D-glucose. *Radiology.* 1991;179:765-70.
27. Takamochi K, Nagai K, Yoshida J, et al. Pathologic N0 status in pulmonary adenocarcinoma is predictable by combining serum carcinoembryonic antigen level and computed tomographic findings. *J Thorac Cardiovasc Surg.* 2001;122:325-30.
28. Higashi K, Ueda Y, Seki H. F-18 FDG PET imaging is negative in bronchiolo-alveolar lung carcinoma. *J Nucl Med.* 1998;39:1016-20.
29. Ginsberg RJ, Rubinstein LV. Randomized trial of lobectomy versus limited resection for T1N0 non-small cell lung cancer. Lung Cancer Study Group. *Ann Thorac Surg.* 1995;60:615-22.
30. Ichinose Y, Yano T, Yokoyama H, Inoue T, Asoh H, Katsuda Y. The correlation between tumor size and lymphatic vessel invasion in resected peripheral stage I non-small cell lung cancer. A potential risk of limited resection. *J Thorac Cardiovasc Surg.* 1994;108:684-6.
31. Naruke T, Tsuchiya R, Kondo H, Nakayama H, Asamura H. Lymph node sampling in lung cancer: how should it be done? *Eur J Cardiothorac Surg.* 1999;16(suppl):S17-24.
32. Asamura H, Nakayama H, Kondo H, Tsuchiya R, Naruke T. Lobe-specific extent of systemic lymph node dissection for non-small cell lung carcinomas according to a retrospective study of metastases and prognosis. *J Thorac Cardiovasc Surg.* 1999;117:1102-11.
33. Liptay MJ, Masters GA, Winchester DJ, et al. Intraoperative radioisotope sentinel lymph node mapping in non-small cell lung cancer. *Ann Thorac Surg.* 2000;70:384-90.
34. Nomori H, Horio H, Naruke T, Orikasa H, Yamazaki K, Suemasu K. Use of technetium-99m tin colloid for sentinel lymph node identification in non-small cell lung cancer. *J Thorac Cardiovasc Surg.* 2002; 124:486-92.

GTS

Progression of Focal Pure Ground-Glass Opacity Detected by Low-Dose Helical Computed Tomography Screening for Lung Cancer

Ryutaro Kakinuma, MD, Hironobu Ohmatsu, MD, Masahiro Kaneko, MD, Masahiko Kusumoto, MD, Junji Yoshida, MD, Kanji Nagai, MD, Yutaka Nishiwaki, MD, Toshiaki Kobayashi, MD, Ryosuke Tsuchiya, MD, Hiroyuki Nishiyama, MD, Eisuke Matsui, MD, Kenji Eguchi, MD, and Noriyuki Moriyama, MD

Objective: To clarify the progression of focal pure ground-glass opacity (pGGO) detected by low-dose helical computed tomography (CT) screening for lung cancer.

Methods: A total of 15,938 low-dose helical CT examinations were performed in 2052 participants in the screening project, and 1566 of them were judged to have yielded abnormal findings requiring further examination. Patients with peripheral nodules exhibiting pGGO at the time of the first thin-section CT examination and confirmed histologically by thin-section CT after follow-up of more than 6 months were enrolled in the current study. Progression was classified based on the follow-up thin-section CT findings.

Results: The progression of the 8 cases was classified into 3 types: increasing size (n = 5: bronchioloalveolar carcinoma [BAC]), decreasing size and the appearance of a solid component (n = 2: BAC, n = 1; adenocarcinoma with mixed subtype [Ad], n = 1), and stable size and increasing density (n = 1: BAC). In addition, the decreasing size group was further divided into 2 subtypes: a rapid-decreasing type (Ad: n = 1) and a slow-decreasing type (BAC: n = 1). The mean period between the first thin-section CT and surgery was 18 months (range: 7–38 months). All but one of the follow-up cases of lung cancer were noninvasive whereas the remaining GGO with a solid component was minimally invasive.

Conclusions: The pGGOs of lung cancer nodules do not only increase in size or density, but may also decrease rapidly or slowly with the appearance of solid components. Close follow-up until the appearance of a solid component may be a valid option for the management of pGGO.

Key Words: ground-glass opacity, low-dose helical computed tomography screening, lung cancer

(*J Comput Assist Tomogr* 2004;28:17–23)

Focal pure ground-glass opacities (pGGOs), or nodules of the lungs, has become a major concern as low-dose helical computed tomography (CT) screening for lung cancer becomes more widely available, not only in the field of diagnostic imaging,[1–5] but also in the field of limited surgery.[6–10] GGO is a finding on thin-section CT images of the lung which has been described as a hazy, increased attenuation of the lung tissue with preservation of the bronchial and vascular margins. GGO is usually a nonspecific finding that is found in many types of pulmonary disease.[11] However, some investigators have recently reported that most localized pGGOs or focal GGOs are malignant.[1,2,5] Although a few reports have described the evolution of lung cancer using conventional chest CT,[12–14] thin-section CT[15–17] and low-dose screening CT,[18,19] the natural history of peripheral lung cancers that exhibit as pGGO on thin-section CT images detected using low-dose helical CT screening is still unclear.

The purpose of this retrospective study was to clarify the progression of pGGOs, which were not visible on chest radiographs, detected by low-dose helical CT screening examinations performed every 6 months. We evaluated the progression of pGGOs based on the thin-section CT findings obtained during the follow-up after the first thin-section CT.

PATIENTS AND METHODS

Subjects

Between September 1993 and January 2003, low-dose helical CT screening was conducted semiannually in Tokyo by

From the Division of Thoracic Oncology (Drs Kakinuma, Ohmatsu, Yoshida, Nagai, and Nishiwaki), National Cancer Center Hospital East, Tsukiji, Chiba Japan; the Divisions of Endoscopy (Drs Kaneko and Kobayashi), Diagnostic Radiology (Drs Kusumoto and Moriyama), and Thoracic Surgery (Dr Tsuchiya), National Cancer Center Hospital; the Division of Thoracic Surgery (Dr Nishiyama), Social Health Insurance Medical Center, Okubo, Japan; (Dr Matsui); the Anti–Lung Cancer Association, Ichigaya, Japan; and the Division of Internal Medicine (Dr Eguchi), School of Medicine, Tokai University, Isehara, Japan.

This study was supported in part by a Grant-in-Aid for Cancer Research (13-8) from the Ministry of Health, Labor, and Welfare of Japan and by a Grant-in-Aid from the Second-Term Comprehensive 10-Year Strategy for Cancer Control.

Reprints: Ryutaro Kakinuma, MD, National Cancer Center Hospital East, 6-5-1 Kashiwa-no-ha, Kashiwa, Chiba 277-8577, Japan (e-mail: rkaki@east.ncc.go.jp).

the Anti–Lung Cancer Association (ALCA), a for-profit organization for lung cancer screening.[20,21] Each screening consisted of a low-dose helical CT examination, chest radiography, and cytologic sputum studies. During this period, a total of 15,938 low-dose helical CT examinations were performed in 2052 ALCA members. Among the low-dose helical CT examinations, a total of 1566 CT examinations were judged as having abnormal findings requiring further examination. Sixty-seven cases of lung cancer (peripheral-type lung cancer, 61; hilar-type lung cancer, 6) were detected during the ALCA lung cancer screening project. Out of these 67 cases, 51 cases (76%) were pathologic stage IA. The treatments used in the 67 cases were as follows: surgery (n = 55), radiotherapy (n = 5), radiotherapy and chemotherapy (n = 2), chemotherapy (n = 4), and photodynamic therapy (n = 1). Among the patients with peripheral nodules detected by the low-dose helical CT examinations performed every 6 months, the patients with histologically diagnosed nodules exhibiting pGGO larger than 5 mm in diameter at the time of the first thin-section CT and followed-up by thin-section CT for more than 6 months were enrolled in the current study.

CT Scanning Conditions

A TCT900S Superhelix CT scanner (Toshiba Medical Inc., Tokyo, Japan) was used for all of the examinations. Low-dose helical CT screening was performed under the following conditions: 120 kV, 50 mA, beam width of 10 mm, 1 rotation of the x-ray tube per second, and a table speed of 20 mm per second (pitch 2:1). Reconstruction was performed at intervals of 10 mm. The CT images were displayed on a monitor with a window width of 2000 HU and a window level of −700 HU. If newly developed nodules were identified, thin-section CT examinations were performed under the following conditions: 120 kV, 250 mA, beam width of 2 mm, 1 rotation of the x-ray tube per second, and a table speed of 2 mm per second (pitch 1:1). Reconstruction was performed at intervals of 2 mm using a thin-section CT algorithm.

Evaluation of pGGO Progression Patterns

The progression patterns were classified based on changes in the size and density of the pGGOs on the thin-section CT images. The study period was divided into 2 phases: the unidentified phase (ie, the period prior to the first thin-section CT scan) and the follow-up phase (ie, the period after the first thin-section CT scan). CT images of the pGGOs in the unidentified phase were reviewed independently by 4 physicians (R.K., M.K., H.O., K.E.), who are diagnostic experts in chest radiology, and by 1 radiologist (M.K.). CT findings were adopted as positive findings if 3 of more of the doctors agreed. After the independent reviews, we decided by consensus as to how many pGGOs were newly developed or had arisen from inconspicuous nodules during the helical CT screening period. In the follow-up phase, the size of the pGGOs was measured with a pair of calipers on the thin-section CT images obtained during the initial scan and the final scan by consensus of 2 diagnostic experts (R.K., M.K.) to assess doubling time. The size of the lesion was evaluated using measurements that passed through the center of the lesion. Size was defined as the average of the length and width of the lesion. Doubling times were calculated using the Schwartz equation.[22] The density of faint opacities was evaluated visually on the thin-section CT images obtained during the follow-up phase. pGGO was defined as a homogeneous GGO, and mixed GGO was defined as a GGO with a solid component.

Pathologic Classification of Adenocarcinomas

The histologic findings of the adenocarcinomas were classified according to the criteria of the World Health Organization (WHO)[23] and the criteria of Noguchi et al.[24] The classification system for replacement growth patterns developed by Noguchi et al is as follows: type A (localized bronchioloalveolar carcinoma; LBAC), type B (LBAC with foci of collapsed alveolar structure), and type C (LBAC with foci of active fibroblastic proliferation).

RESULTS

Patient Characteristics

Eight patients with pGGOs (6 men and 2 women) were enrolled in the current study (Table 1). The patients ranged in age from 49 to 69 years (mean, 64 years). With regard to smoking history, 3 patients were nonsmokers, 4 were ex-smokers, and 1 was a current smoker. Four of these 8 pGGO patients were not apparent during the initial screening and became apparent during the screening period, and 3 of the other 4 pGGO patients with inconspicuous opacities visible in retrospect during the initial screening became apparent later. In 1 other case, a conspicuous opacity and multiple old tuberculosis lesions were observed during the initial CT screening. The locations of the pGGOs were as follows: right upper lobe (n = 4), right lower lobe (n = 1), left upper lobe (n = 1), and left lower lobe (n = 2).

Clinical Course

The period between the first visible nodule of a pGGO on a thin-section CT image and the first visible opacity on a helical CT screening image when viewed retrospectively ranged from 13 to 46 months (mean, 22 months) (Table 1). The period between the first thin-section CT examination and the surgery ranged from 7 to 39 months (mean, 19 months). The interval between the last thin-section CT examination and surgery ranged from 1 to 98 days (mean, 32 days).

Histology of GGOs

Seven patients had bronchioloalveolar carcinoma (BAC), defined as noninvasive by the WHO classification in 1999, and 1 had an adenocarcinoma with mixed subtypes (Table 1). Based on Noguchi's classification for small adeno-

TABLE 1. Clinical Characteristics and Histology of Ground-Glass Opacities

Case No.	Sex	Age at Detection (Years)	Smoking Index	Development	Lobe	Period Between: First Visible and the First TS-CT (Months)*	Period Between: The First TS-CT and Surgery (Months)*	Period Between: The Last TS-CT and Surgery (Days)	Histology: WHO Classification	Histology: Noguchi Type
1	M	69	1300	New	RU	41	13	1	Ad	C
2	M	69	800 (ex)	New	RU	13	39	36	BAC	B
3	F	66	Non	New	LL	13	14	33	BAC	A
4	M	66	450 (ex)	New	LU	18	26	98	BAC	A
5	F	65	Non	ic	LL	46	28	13	BAC	B
6	M	69	800 (ex)	ic	RU	21	12	13	BAC	A
7	M	49	515 (ex)	ic	RU	14	10	6	BAC	A
8	M	63	Non	c	RL	13	7	57	BAC	B

Non, nonsmoker; ex, ex-smoker; ic, inconspicuous; c, conspicuous; RU, right upper lobe; LU, left upper lobe; LL, left lower-lobe; TS-CT, thin-section CT; BAC, bronchioloalveolar carcinoma; Ad, adenocarcinoma.
*Number of months was rounded.

carcinomas, the pGGOs consisted of 4 cases of type A and 2 cases of type B while the mixed GGOs consisted of 1 case of type B and 1 case of type C (Tables 1, 2). All the lung cancers were diagnosed at pathologic stage IA.

Progression of pGGOs

The period between the first thin-section CT and the final thin-section CT examinations ranged from 6 to 37 months (mean, 17 months) (Table 3). The opacities ranged in size from 6.5 mm to 17 mm (mean, 10 mm) at the time of the first thin-section CT examination and from 7 mm to 16.5 mm (mean, 10.5 mm) at the time of the final thin-section CT examination.

The progressions of 8 opacities in the follow-up phase were classified into 3 types: increasing in size (Increasing type, n = 5), decreasing in size and the appearance of a solid component (decreasing type, n = 2), and stable in size and increasing in density (density type, n = 1). In addition, the decreasing type was classified into 2 subtypes: a rapid-decreasing type (case 1, Fig. 1; decrease in size at the time of the 6-month follow-up) and a slow-decreasing type (case 2, Fig. 2; decrease after follow-up for more than 1 year). All but 1 of the follow-up cases were noninvasive, and the remaining GGO with a solid component was judged to be minimally invasive adenocarcinoma because the size of the collapse fibrosis was only 2 mm in diameter (Fig. 1F).

TABLE 2. Thin-Section CT Findings, Progression Types, and Doubling Time of Ground-Glass Opacities

Case No.	Follow-Up Phase with Thin-Section CT: GGO Size (mm) First	GGO Size (mm) Final	Final TS-CT of GGO: Density	Solid	Finding	Progression Type	Period of Follow-Up with TS-CT (Months)*	GGO Doubling Time (Days)
1	17	12	Increasing	+	Mixed	Dec	12	−214
2	14	12	Increasing	+	Mixed	Dec	37	−1680
3	6.5	7.5	Stable	−	Pure	Inc	13	617
4	7	10.5	Stable	−	Pure	Inc	22	383
5	7	7	Increasing	−	Pure	Den	27	—
6	8.5	9.5	Stable	−	Pure	Inc	12	669
7	6.5	9	Stable	−	Pure	Inc	10	216
8	13.5	16.5	Stable	−	Pure	Inc	6	198

CT, computed tomography; GGO, ground-glass opacity; TS-CT, thin-section computed tomography; Inc, increasing; Dec, decreasing; Den, density.
*Number of months was rounded.

TABLE 3. Evolution of Solid Components in Ground-Glass Opacities

Case No.	Follow-Up Phase with TS-CT Solid Size (mm) First TS-CT	Months After the First TS-CT 6	11	23	36	Doubling Time (Days)
1	0*	8				14*
2	0	—	2	3	7.5	130†

TS-CT, thin-section computed tomography.

*Doubling time of solid component in case 1 was calculated on the assumption that the first size was 0.5 mm.

†Doubling time of solid component in case 2 was calculated based on the sizes between 11 months and 36 months after the first TS-CT.

Doubling Time

The doubling times of the increasing-type opacities ranged from 198 to 669 days (mean ± SD, 417 ± 220 days). The doubling time of the density-type opacity could not be calculated because it did not change in size. For the decreasing-type opacities, the doubling times were calculated based on the sizes of the pGGOs and the solid components, individually. In case 1, the doubling times of the pGGO and the solid component were −214 and 14 days, respectively. In case 2, the doubling times of the pGGO and the solid component were 1680 and 130 days, respectively.

Correlation of Thin-Section CT Images and Pathologic Findings

The pGGO corresponded to the lepidic growth of cancer cells (Fig. 1E), the thickening of the alveolar wall (Fig. 1E), and the collapse of the alveolar space (Fig. 1E). Solid components corresponded not only to the collapse of the alveolar space and fibrosis (Fig. 1F and Fig. 2G), but also to a severe narrowing of the alveolar space (Fig. 1F). With the development of a solid component in case 2, the distance between the surrounding pulmonary veins and the bronchus gradually narrowed (Figs. 2C–F). The same finding was observed in case 1 (Figs. 1C, D).

DISCUSSION

To our knowledge, this study is the first report to describe the progression of pGGOs in minute lung cancers that appeared as new pGGOs during the screening process or arose from inconspicuous minute nodules on low-dose helical CT screening images obtained at 6-month intervals. In addition, the progressions of the pGGOs on the thin-section CT images were classified into 3 types for the first time. Although a few papers have described the natural history of GGOs in pulmonary adenocarcinoma,[4,7,12,15–17] only 1 researcher[15] reported 2 GGOs that decreased in size, but the size reduction occurred in mixed GGOs, not in pGGOs. The rapid decreasing of a pGGO and the appearance of a solid component has not previously been reported.

Radiologic-pathologic correlations revealed that pGGOs on thin-section CT images mainly represent the lepidic growth of adenocarcinomas.[1,3,4,12,15–17] Solid components in the mixed GGOs were caused by the collapse of alveolar spaces or regions of fibrosis[12] and by a severe narrowing of the alveolar space (case 1). The narrowing of the distance between the surrounding pulmonary vessels and the bronchus was caused not only by the collapse of the alveolar space (cases 1 and 2), but also by the development of fibrosis (case 1) in the pGGO lesions. This finding has been termed "vessel convergence."[12,15,17] Based on our observations of the progression from a pure GGO to a mixed GGO in cases 1 and 2, our results also support the stepwise progression of replacement-type adenocarcinoma.[12,15,17]

Although 1 researcher raised serious questions about the concept of 2-year stability implying benignity,[25] pulmonary nodules are generally considered to be benign if they remain the same size or decrease in size over a 2-year observation period.[26,27] However, our results show that stability or reduction in size over a 2-year period does not necessarily indicate benignity. In the case of a pGGO that decreases in size, can the Schwartz equation be applied to a change from a pGGO to a mixed GGO if the area of the GGO decreases? Usually, the Schwartz equation is based on the assumption that constant exponential tumor growth is the basic pattern of neoplastic proliferation.[22] The doubling time for mixed GGOs has been reported to be 457 ± 260 days.[28] However, progression to a mixed GGO in a case where the pGGO decreases in size and a solid component simultaneously appears has not previously been reported. Moreover, the calculation of doubling times for each component in a mixed GGO has never, to the best of our knowledge, been performed prior to the current study. The doubling time for the solid component in case 1 was calculated based on the assumption that the initial size of the solid component was 0.5 mm, this because the thin-section CT images were taken not only by the single-slice CT scanner described above, but by a multislice CT scanner with the imaging parameters set at 0.5 mm × 4 rows and image reconstruction performed at 1-mm intervals.

Whether pGGOs should be resected or followed up is controversial. Definite evidence of the natural history of pGGOs does not exist at present. However, based on the indirect corroboration described below, we suggest that close follow-up until the appearance of a solid component may be a valid option for the management of pGGO. First, most pGGOs are either atypical adenomatous hyperplasia (preinvasive lesions according to the 1999 WHO criteria), BAC (a noninvasive lesion), or minimally invasive adenocarcinoma.[1,8,29] Second, 1 researcher[7] has previously reported information concerning

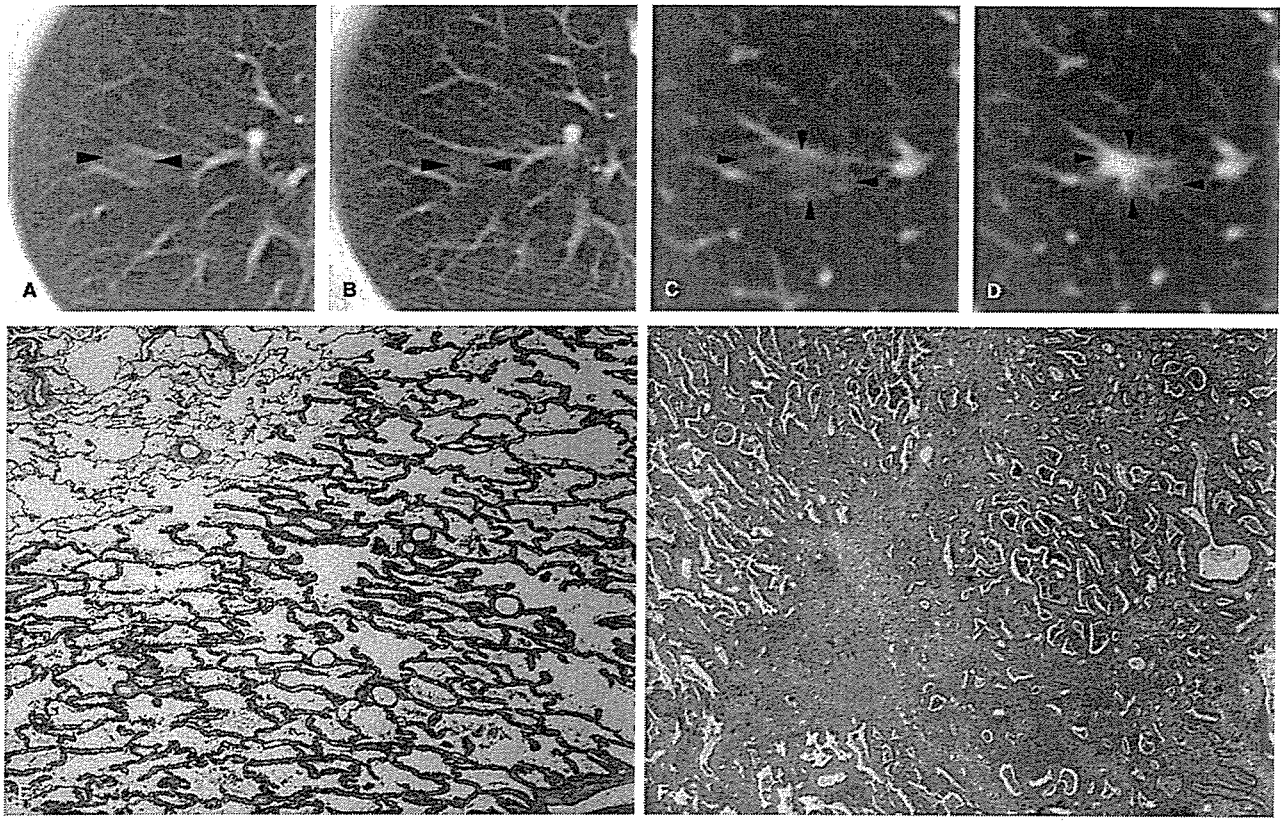

FIGURE 1. Case 1: Adenocarcinoma in a 69-year-old man. A, A faint localized increase in density was identified in segment 1 of the right upper lobe of the lung on a CT screening image obtained in December 2001. B, In retrospect, the opacity was also present on a CT screening image obtained in June 1998. C, Thin-section CT image obtained in December 2001 showing a pGGO in segment 1 of the right upper lobe of the lung. D, Thin-section CT image obtained in June 2002 shows a decrease in the size of the pGGO and the appearance of a solid component. E, Medium-magnification image of the pathologic specimen (H&E staining, ×40). Thickening of the alveolar walls as a result of the tumor cells is visible. F, Medium-magnification image of the pathologic specimen (H&E staining, ×40). Severe narrowing of the alveolar space from the thickening of the alveolar walls and an area of collapse-fibrosis with active fibroblastic proliferation are visible. A right upper lobectomy was performed in January 2003. The lesion was diagnosed as an adenocarcinoma, 17 mm in diameter (Noguchi type C). The size of collapse- fibrosis was 2 mm in diameter.

the natural history of pGGOs after conducting a long-term follow-up study lasting more than 2 years. Five of the 19 cases of pGGOs were diagnosed as lung cancers, that is, 5 BACs (1 case had 2 BACs) and 1 adenocarcinoma, after a mean follow-up of 61 months. Although the patient with adenocarcinoma was followed up for 124 months, personal communication with the author revealed that his lung cancer was of pathologic stage IA and that the size of the central fibrosis of the adenocarcinoma was less than 3 mm in diameter. We have also experienced 2 other pGGOs that developed into mixed GGOs after a 1-year and a 3-year follow-up period, respectively (unpublished data). These lesions were diagnosed as pathologic stage IA adenocarcinomas, and the size of the central fibrosis was 1.5 mm and 2 mm in diameter, respectively. Regarding the relationship between central fibrosis and prognosis, our research team[30] previously reported that 21 out of 100 patients with a lung adenocarcinoma that was 3 cm or less in diameter and which had a central fibrosis of 5 mm or less in diameter had a 5-year survival rate of 100%. Therefore, the adenocarcinoma follow-up cases described above and in this study were thought to be minimally invasive, allowing the possibility of a cure. Third, the adenocarcinoma cases with mixed GGOs did not experience any relapses or deaths, even though the solid components of the GGOs became larger but remained less than 50% of the mixed GGO nodule, this from the standpoint of the GGO's length,[31] the vanishing ratio of GGO[10] ("air-containing type"), and the volume of the GGO.[9] Finally, adenocarcinoma pGGOs tend to grow slowly, as the mean doubling time of pGGOs has been reported to be 813 days[28] or 880 days.[12] In addition, one-fourth of the GGOs in 1 study were

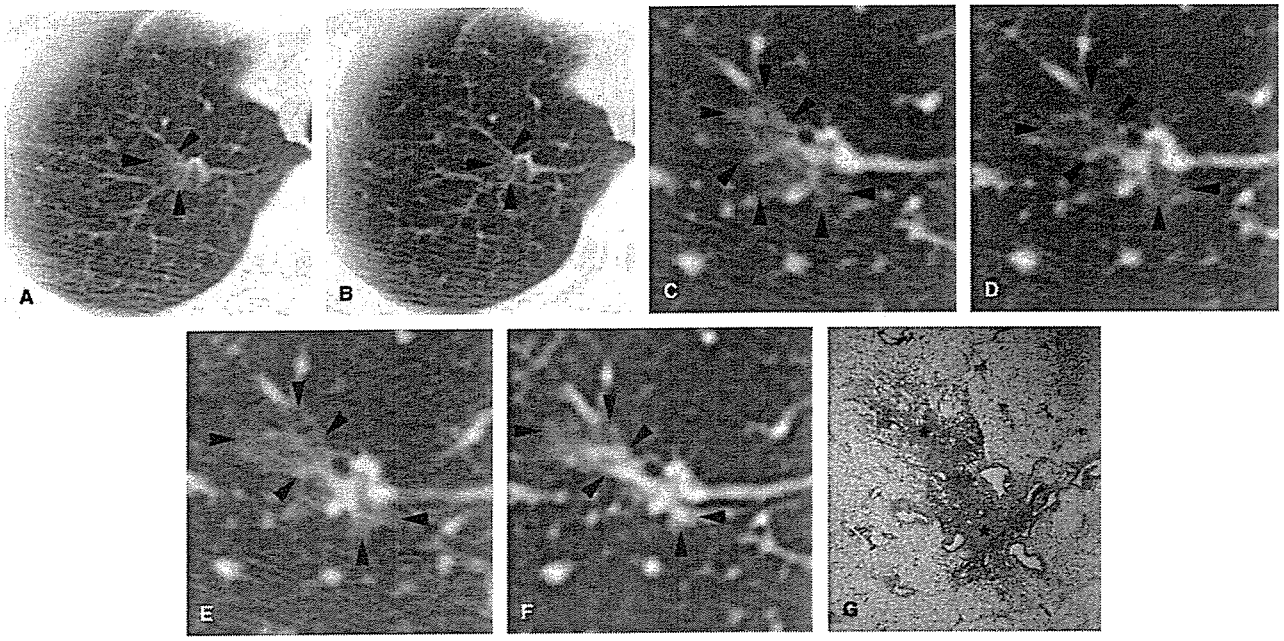

FIGURE 2. Case 2: Bronchioloalveolar carcinoma in a 69-year-old man. A, A faint localized increase in density was identified in segment 1 of the right upper lobe of the lung on a CT screening image obtained in February 1999. B, In retrospect, the opacity was also visible on a CT screening image obtained in February 1998. C, Thin-section CT revealed a pGGO in segment 1 of the right upper lobe of the lung in March 1999. D, Thin-section CT image obtained in February 2000 showing a pGGO with a small solid component. E, Thin-section CT image obtained in February 2001 showing a decrease in the size of the pGGO and a slight increase in the size of the solid component. F, Thin-section CT image obtained in February 2002 showing a larger decrease in the size of the pGGO and an increase in the size of the solid component. G, Low-magnification image of the pathologic specimen (H&E staining, ×5). The foci of alveolar collapse (asterisks) are shown. A right upper lobectomy was performed in May 2002. The lesion was diagnosed as a bronchioloalveolar carcinoma, 15 mm in diameter (Noguchi type B).

stable after a mean follow-up period of 16 months,[17] whereas half of the pGGOs in another study showed no change in size after a median follow-up period of 32 months.[7] Therefore, the classification of some pGGOs may be affected by an overdiagnosis bias.

This study has some limitations. First, the period of pGGO development was not accurately assessed because only thick-sectioned screening CT images were available for the unidentified phase. Therefore, the partial volume effect affected the detectability of small faint opacities on screening CT images. Multislice CT imaging using a narrow collimation and thinner reconstruction images may reveal the natural history of pGGOs more precisely. Second, measurements made with a pair of calipers to calculate doubling times may lead to measurement errors. Although technical advances have been reported,[32,33] we did not have any commercial software for volume measurements. Third, our study cohort was very small. At the start of the helical CT screening project, surgery without follow-up tended to be recommended in cases with pGGO. After knowledge of pGGOs had accumulated (ie, that most pGGOs consisted of preinvasive, noninvasive, or minimally invasive lesions), our treatment procedure changed.[8] Now, resection is only 1 option, not the only option, as in the past. Because of this, resection data cannot always be obtained, and the number of cases was small as a result.

In conclusion, the natural history of pGGOs detected by helical CT screening for lung cancer was partially revealed. A classification for pGGO progression was proposed based on thin-section CT images obtained during the follow-up phase. The pGGOs of lung cancer nodules do not only increase in size or density, but may also decrease rapidly or slowly with the appearance of solid components. Close follow-up until the appearance of a solid component may be a valid option for the management of pGGO.

ACKNOWLEDGMENTS

The authors thank Fumio Shishido, MD, PhD (Department of Radiology, School of Medicine, Fukushima Medical University) for his encouragement. We also wish to thank the pathologists who assisted in this study: Yoshihiro Matsuno, MD (National Cancer Center Research Institute), Tomoyuki Yokose, MD, and Genichiro Ishii, MD (National Cancer Center Research Institute East). We also thank the physicians, the

technical staff, and the administrative staff of the Anti–Lung Cancer Association in Tokyo.

REFERENCES

1. Nakajima R, Yokose T, Kakinuma R, et al. Localized pure ground-glass opacity on high-resolution CT: histologic characteristics. *J Comput Assist Tomogr*. 2002;26:323–329.
2. Nakata M, Saeki H, Takata I, et al. Focal ground-glass opacity detected by low-dose helical CT. *Chest*. 2002;121:1464–1467.
3. Kuriyama K, Seto M, Kasugai T, et al. Ground-glass opacity on thin-section CT: value in differentiating subtypes of adenocarcinoma of the lung. *AJR Am J Roentgenol*. 1999;173:465–469.
4. Yang ZG, Sone S, Takashima S, et al. High-resolution CT analysis of small peripheral lung adenocarcinomas revealed on screening helical CT. *AJR Am J Roentgenol*. 2001;176:1399–1407.
5. Henschke CI, Yankelevitz DF, Mirtcheva R, et al. CT screening for lung cancer: frequency and significance of part-solid and nonsolid nodules. *AJR Am J Roentgenol*. 2002;178:1053–1057.
6. Kodama K, Higashiyama M, Yokouchi H, et al. Prognostic value of ground-glass opacity found in small lung adenocarcinoma on high-resolution CT scanning. *Lung Cancer*. 2001;33:17–25.
7. Kodama K, Higashiyama M, Yokouchi H, et al. Natural history of pure ground-glass opacity after long-term follow-up of more than 2 years. *Ann Thorac Surg*. 2002;73:386–393.
8. Suzuki K, Asamura H, Kusumoto M, et al. "Early" peripheral lung cancer: prognostic significance of ground-glass opacity on thin-section computed tomographic scan. *Ann Thorac Surg*. 2002;74:1635–1639.
9. Matsuguma H, Yokoi K, Anraku M, et al. Proportion of ground-glass opacity on high-resolution computed tomography in clinical T1N0M0 adenocarcinoma of the lung: a predictor of lymph node metastasis. *J Thorac Cardiovasc Surg*. 2002;124:278–284.
10. Kondo T, Yamada K, Noda K, et al. Radiologic-prognostic correlation in patients with small pulmonary adenocarcnomas. *Lung Cancer*. 2002;36: 49–57.
11. Austin JM, Muller NL, Friedman PJ, et al. Glossary of terms for CT of the lung: recommendations of the Nomenclature Committee of the Fleischner Society. *Radiology*. 1996;200:327–331.
12. Aoki T, Nakata H, Watanabe H, et al. Evolution of peripheral lung adenocarcinomas: CT findings correlated with histology and tumor doubling time. *AJR Am J Roentgenol*. 2000;174:763–768.
13. White CS, Romney BM, Mason AC, et al. Primary carcinoma of the lung overlooked at CT: analysis of findings in 14 patients. *Radiology*. 1996; 199:109–115.
14. Gurney JW. Missed lung cancer at CT: imaging findings in nine patients. *Radiology*. 1996;199:117–122.
15. Koizumi N, Sakai K, Matsuzuki Y, et al. Natural history of cloudy zone of pulmonary adenocarcinoma on HRCT [in Japanese]. *Nippon Igaku Hoshasen Gakkai Zasshi*. 1996;56:715–719.
16. Jang HJ, Lee KS, Kwon OJ, et al. Bronchioloalveolar carcinoma: focal area of ground-glass attenuation at thin-section CT as an early sign. *Radiology*. 1996;199:485–488.
17. Takashima S, Maruyama Y, Hasegawa M, et al. CT findings and progression of small peripheral lung neoplasms having a replacement growth pattern. *AJR Am J Roentgenol*. 2003;180:817–826.
18. Kakinuma R, Ohmatsu H, Kaneko M, et al. Detection failures in spiral CT screening for lung cancer: analysis of CT findings. *Radiology*. 1999;212: 61–66.
19. Li F, Sone S, Abe H, et al. Lung cancers missed at low-dose helical CT screening in a general population: comparison of clinical, histopathologic, and imaging findings. *Radiology*. 2002;225:673–683.
20. Kaneko M, Eguchi K, Ohmatsu H, et al. Peripheral lung cancer: screening and detection with low-dose spiral CT versus radiography. *Radiology*. 1996;201:798–802.
21. Sobue T, Moriyama N, Kaneko M, et al. Screening for lung cancer with low-dose helical computed tomography: Anti–Lung Cancer Association project. *J Clin Oncol*. 2002;20:911–920.
22. Schwartz M. A biomathematical approach to clinical tumor growth. *Cancer*. 1961;14:1272–1294.
23. Travis W, Colby T, Corrin B, et al. *Histological Typing of Lung and Pleural Tumors*. Berlin: Springer; 1999.
24. Noguchi M, Morikawa A, Kawasaki M, et al. Small adenocarcinoma of the lung: histologic characteristics and prognosis. *Cancer*. 1995;75:2844–2852.
25. Yankelevitz DF, Henschke CI. Does 2-year stability imply that pulmonary nodules are benign? *AJR Am J Roentgenol*. 1997;168:325–328.
26. Swensen SJ, Jett JR, Hartman TE, et al. Lung cancer screening with CT: Mayo Clinic experience. *Radiology*. 2003;226:756–761.
27. Benjamin MS, Drucker EA, McLoud TC, et al. Small pulmonary nodules: detection at chest CT and outcome. *Radiology*. 2003;226:489–493.
28. Hasegawa M, Sone S, Takashima S, et al. Growth rate of small lung cancers detected on mass CT screening. *Br J Radiol*. 2000;73:1252–1259.
29. Nakata M, Sawada S, Saeki H, et al. Prospective study of thoracoscopic limited resection for ground-glass opacity selected by computed tomography. *Ann Thorac Surg*. 2003;75:1601–1606.
30. Suzuki K, Yokose T, Yoshida J, et al. Prognostic significance of the size of central fibrosis in peripheral adenocarcinoma of the lung. *Ann Thorac Surg*. 2000;69:893–897.
31. Aoki T, Tomoda Y, Watanabe H, et al. Peripheral lung adenocarcinoma: correlation of thin-section CT findings with histologic prognostic factors and survival. *Radiology*. 2001;220:803–809.
32. Yankelevitz Df, Reeves AP, Kostis WJ, et al. Small pulmonary nodules: volumetrically determined growth rates based on CT evaluation. *Radiology*. 2000;217:251–256.
33. Ko JP, Rusinek H, Jacobs EL, et al. Small pulmonary nodules: volume measurement at chest CT-phantom study. *Radiology*. 2003;228:864–870.

Reprinted from
Jpn J Clin Oncol 2005;35(11)667–671
doi:10.1093/jjco/hyi177

A Flexible Endoscopic Surgical System: First Report on a Conceptual Design of the System Validated by Experiments

Toshiaki Kobayashi[1], Sean Lemoine[1,2], Akihiko Sugawara[1,2], Takaaki Tsuchida[1], Takuji Gotoda[1], Ichiro Oda[1], Hirohisa Ueda[3] and Tadao Kakizoe[1]

[1]National Cancer Center, [2]Japan Association for the Advancement of Medical Equipment and [3]Pentax Corporation, Tokyo, Japan

Jpn J Clin Oncol 2005;35(11)667–671
doi:10.1093/jjco/hyi177

A Flexible Endoscopic Surgical System: First Report on a Conceptual Design of the System Validated by Experiments

Toshiaki Kobayashi[1], Sean Lemoine[1,2], Akihiko Sugawara[1,2], Takaaki Tsuchida[1], Takuji Gotoda[1], Ichiro Oda[1], Hirohisa Ueda[3] and Tadao Kakizoe[1]

[1]National Cancer Center, [2]Japan Association for the Advancement of Medical Equipment and [3]Pentax Corporation, Tokyo, Japan

Received May 17, 2005; accepted August 25, 2005; published online November 8, 2005

Background: Surgery is a standard diagnostic and therapeutic procedure. However, its technical difficulty and invasiveness pose problems that are yet to be solved even by current surgical robots. Flexible endoscopes can access regions deep inside the body with less invasiveness than surgical approaches. Conceptually, this ability can be a solution to some of the surgical problems.
Methods: A flexible (surgical) endoscopic surgical system was developed consisting of an outer and two inner endoscopes introduced through two larger working channels of the outer endoscope. The concept of the system as a surgical instrument was assessed by animal experiments.
Results: Gastric mucosa of the swine could be successfully resected using the flexible endoscopic surgical system, thereby showing us the prospect and directions for further development of the system.
Conclusion: The concept of a flexible endoscopic surgical system is considered to offer some solutions for problems in surgery.

Key words: surgical robot – endoscopic surgery – surgery – robotics – endoscope

INTRODUCTION

We recently reported a new concept for endoscopic mucosal resection of gastric cancer with the use of a magnetic anchor. The anchor consisted of microforceps and a magnetic weight in order to grasp, stabilize and pull up the gastric mucosa (1). During the experiments, we thought that the procedure would be easier if one more endoscope was present to hold and stabilize the mucosa instead of the magnetic anchor.

Concerning flexible endoscopes, there are some ultrathin endoscopes that can be inserted into the working channels of standard endoscopes, such as gastrointestinal endoscopes. If the outer endoscope is able to contain larger and multiple working channels, several thin endoscopes could be inserted through the outer endoscope. This would allow for the resecting procedures. Such a system could also be applied to the fields where current surgical robots are targeting.

One of the problems with current surgical robots is inaccessibility to regions located deep inside the body, particularly regions reached through narrow and winding routes, such as the digestive tracts and blood vessels. However, some early gastric cancers can be resected endoscopically with much less invasiveness than surgery. These surgeries cannot be performed by current surgical robot systems because those regions were not originally considered places for the systems to operate.

An experimental flexible endoscopic surgical system was developed to cope with these problems of accessibility, consisting of a flexible outer endoscope with two working channels through which two inner flexible endoscopes could be inserted. These inner endoscopes were designed to have similar functions as flexible gastrointestinal endoscopes allowing for performance of standard endoscopic procedures even when introduced through the outer endoscope.

The uses of the flexible endoscopic system as a surgical instrument, as well as its functionality, were confirmed during gastric mucosal resection of the swine. This is in contrast to the current limitations for surgical robotics in terms of lesion access.

MATERIALS AND METHODS

Flexible Surgical Endoscope

As shown in Fig. 1, the flexible surgical endoscope consists of an outer flexible endoscope and two inner flexible endoscopes inserted into the working channel of the outer endoscope. The specifications of these endoscopes are listed in Table 1.

For reprints and all correspondence: Toshiaki Kobayashi, Cancer Screening Technology Division, Research Center for Cancer Prevention and Screening, National Cancer Center, 1-1, Tsukiji 5-chome, Chuo-ku, Tokyo 104-0045, Japan. E-mail: tkobayas@ncc.go.jp

The outer endoscope also has a 2.8 mm working channel and a charge coupled device (CCD) enabling the endoscope to operate in a similar fashion as standard gastrointestinal endoscopes. The endoscopic images are observed on cathode ray tube (CRT) monitors in the same manner as video-endoscopes.

Each of the inner endoscopes has a 2.0 mm working channel allowing accessories such as forceps and an electrocautery tip to be introduced and used. Unlike the outer endoscope, the inner endoscopes have optic fiber bundles for image visualization, instead of a CCD. These endoscopic images are also observed on CRT monitors. However, a video-adaptor, i.e. a small CCD video camera, must be connected onto each eye piece of the inner endoscopes in order to view the image on the monitors.

These combined endoscopes are manipulated manually by three physicians together with the help of several assistants. The system, as a whole, operates similar to surgical robotic systems.

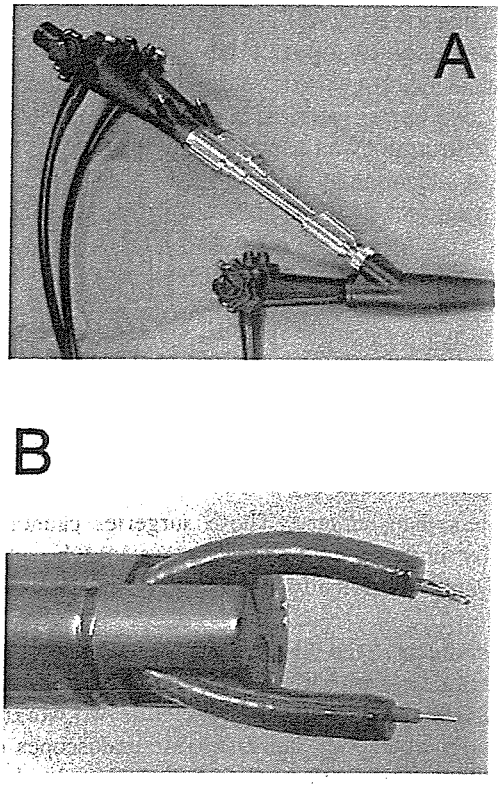

Figure 1. The flexible endoscopic surgical system. (A) The inner endoscope is inserted through a telescopic connecting device, which connects to the opening for the working channel of the outer endoscope near its control section. (B) At the tip of the outer endoscope two inner endoscopes protrude laterally, obtaining a certain distance between the two endoscopes.

Table 1. Specifications of the flexible endoscopic surgical system

	Outer endoscope	Inner endoscope
Total length (mm)	975	1395
Working length (mm)	665	1050
Insertion portion diameter (mm)	20	4.9
Tip bending (degree) (up/down, right/left)	210/120, 120/120	210/120, 120/120
Field of view (degree)	140	120
Depth of field (mm)	4–100	3–50
Channel diameter (mm)	7, 7, 2.8	2

PHYSICIANS

Two series of experiments were conducted. The first series was performed by a senior endoscopist and three resident physicians in order to assess the system with consideration to its endoscopic nature. The senior endoscopist was trained within the specialty of internal medicine, whereas one of the resident physicians was in training for internal medicine and the other two were for surgery.

The purpose of the subsequent series was to assess the concept of the flexible surgical endoscope from the viewpoint of surgeons. Consequently, the procedure was performed by two senior endoscopists, one having more than 15 year experience as a surgeon and the other having some surgical training, in addition to two residents who were in training for surgery.

These two series were performed on separate occasions, with none of the physicians performing in both series.

TEST SUBJECT

Three female swine, under intravenous anesthesia, were laid on an examination table in the left lateral position. Within the first experiment, a 35.6 kg and a 34.1 kg swine were used. In the following experiment, a 41.8 kg swine was used. During these experiments, the law for the humane treatment and management of animals was observed.

PROCEDURE

The procedure was similar to standard endoscopic mucosal resection with the exception of one more endoscope for stabilization of the gastric mucosa.

First, an incision was made in the mucosa surrounding the region of stomach intended for resection (2,3). The outer endoscope was inserted through the esophagus into the gastric cavity. Subsequently, using the telescopic connecting devices (Fig. 1), the inner endoscopes were inserted into the working channels of the outer endoscope and introduced into the gastric cavity.

The outer endoscope was placed near the region in which the first incision was made. Thereafter, the resecting procedure was performed using an electrosurgical knife through one of the working channels of the inner endoscopes, whereas the other contained forceps. Within the procedure, the operator decided which side of the working channels would use the electrosurgical knife.

These procedures were observed on three CRT monitors, each of which was connected to its endoscopic counter part.

The resecting procedures were performed on the anterior wall of the gastric angle, the anterior wall of the middle gastric body and the greater curvature of the middle gastric body in the

first series for the assessment of endoscopic features. Within the following series, the resecting procedures were performed on two regions adjacent to the greater curvature of the lower gastric body.

RESULTS

Concerning insertion of the outer endoscope through the esophagus into the gastric cavity, some difficulties were encountered owing to the large diameter of the outer endoscope and the relatively small size of the swine in both experimental series. However, the outer endoscope was introduced into the gastric cavity.

As for insertion of the inner endoscopes through the working channels of the outer endoscope, there were no difficulties experienced, even when the outer endoscope was bent due to insertion through the esophagus. Access to regions of the gastric wall was limited to the greater curvature due to the rigidity of the outer endoscope.

Maneuverability of the flexible endoscopic surgery system was satisfactory regarding the experiments were the first experiences for the physicians involved, despite some problems to solve.

The images from the outer endoscope were similar to those of standard gastrointestinal video-endoscopes due to the CCD system used in the outer endoscope. However, the images from the inner endoscopes were inferior to those of the outer endoscope. This inferiority was attributed to the limited number of optical fibers within the inner endoscope and deterioration of the image caused by conversion from optical images to electrical images through the use of a video-adapter. Consequently, during most of the procedure, endoscopic images were mainly observed using the monitor for the outer endoscope.

Some differences in use of the inner endoscopes for the resecting procedures between the first series and the second series were noticed. In the first series, the physicians appeared to have difficulties in some of the procedures such as accessing the mucosa, stabilization of the mucosal flap and resection procedures. These procedures were considered standard techniques for actual surgery, which means surgical experiences are required even to maneuver the flexible endoscopic surgical system.

Within the second series conducted by endoscopists with surgical experience, the resecting procedures were satisfactory, despite the fact this was their first experience using the system (Fig. 2). Through cooperation between the operator and assistants using verbal commands, manipulation of the inner endoscopes and the outer endoscope could be achieved. The functions of the inner endoscopes could be modified by changing the instruments inserted into the working channels. The flexible nature of the inner endoscopes allowed additional functions such as stabilization of the gastric wall by the longitudinal flank of the endoscope, as shown in Fig. 2C.

Within all the experiments, resecting procedures were completed without any complications such as perforation of the gastric wall. Consequently, five mucosal pieces, with sizes of

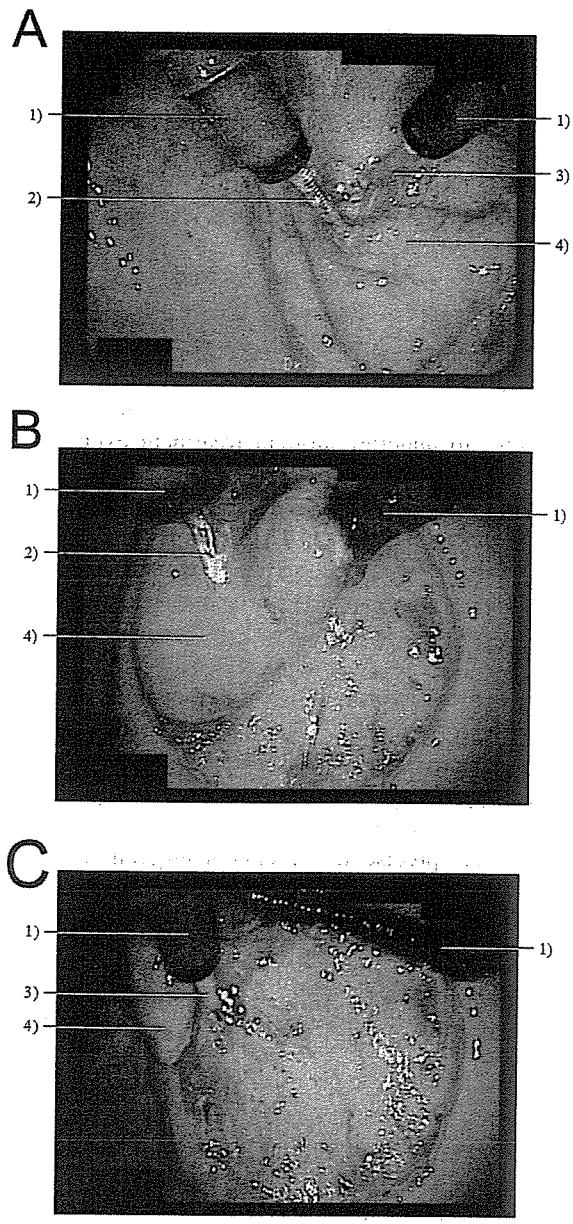

Figure 2. Images of the resecting procedures. (1) Inner endoscope, (2) forceps, (3) electrosurgical knife and (4) mucosal flap. (A) The right inner endoscope, with an electrosurgical knife introduced through its working channel, was maneuvered by the operator. The left inner endoscope, with forceps, was maneuvered by an assistant. (B) The tip of the right inner endoscope is holding up the mucosal flap in order to assist the forceps of the left inner endoscope to grasp the mucosal flap. (C) The right inner endoscope is pulling up the mucosal flap using forceps concealed in this image. In addition, using the flexibility of the endoscope, the gastric wall is stabilized by the longitudinal flank of the inner endoscope.

2.8×1.6 cm^2, 2.8×2.7 cm^2 and 2.6×2.0 cm^2 in the first series, and 3.2×2.7 cm^2 and 4.0×3.4 cm^2 in the second series were each resected in a single piece.

DISCUSSION

Surgical procedures are good options for diagnosis and treatment providing several advantages over non-surgical

approaches, especially in cases of malignant diseases. Although surgery is well accepted as a standard procedure in medicine there are still some problems left unsettled.

The technical difficulty of surgery is a common problem particularly for trainees, but even for experienced surgeons who have some technical limitations. Surgical procedures are difficult for regions deep in the body because the visual field for surgeons is limited, the number of surgical instruments which can be introduced is limited and the movements of these instruments are limited. One of the exemplary regions of this problem is the pelvic cavity, which includes surgery of rectal and prostate cancers.

Invasiveness is an inherent drawback to surgery, discouraging patients to undergo surgical treatment even when it is appropriate. It is true that surgery should be avoided when there are other less invasive alternatives.

Surgical robots such as the da Vinci system and the Zeus system are highly advanced medical instruments allowing for fine movements when appropriately manipulated by surgical experts. These systems are expected to solve some surgical problems such as invasiveness and the difficulty (4–8). Thus far, the systems have been able to solve some of the problems associated with surgery.

As for the invasiveness of surgery, endoscopic surgeries such as laparoscopy can be performed with robotic systems, utilizing smaller incisions than those of other standard open surgical approaches. The precise movements of surgeons are facilitated by robotic systems. However, laparoscopic procedures can be performed even without the robotic systems with the same amount of invasiveness.

Current robotic systems may also pose problems (4–8), such as the limited number of surgeons who can manipulate the system, which is usually one. Additional training for the specific manipulating methods of the systems is another problem, as well as introduction costs. Consequently, it is currently not clear what the benefits of these robotic systems are, especially when assessed from the patient side. Moreover, problems which even surgical experts suffer from have not been solved.

Flexible endoscopes have been developed to cope with the problems of accessing regions through narrow tracts such as the esophagus and the tracheobronchial tree. Even in these regions flexible endoscopes can perform surgical procedures similar to standard surgery. Therefore, endoscopes are naturally considered functional even in other cavities such as the abdomen and pelvic cavities.

It would be easier and more functional to perform an operation using several endoscopic instruments introduced through the end of one endoscope, rather than conducting resection using only one endoscopic instrument introduced into one endoscope, as done in standard endoscopic procedures. The simplest model for this concept is the flexible endoscopic surgical system we developed and examined within these trials.

We assumed that there would be several problems with the flexible endoscopic surgical system when used clinically as it is merely a conceptual model to confirm its feasibility of use. However, despite those problems, the system was able to perform surgical resection. In addition, the problems encountered within the first experiment were inherent in all technical procedures.

Of interest, these problems showed us that, when indicated for resecting procedures, the flexible endoscopic surgical system is easier to manipulate by surgeons and not by endoscopists despite its endoscopic appearances.

The images of the inner endoscopes were not satisfactory because a CCD was not used in these endoscopes. Consequently, resecting procedures were monitored by images from the outer endoscope which contained the CCD. In this situation, the operator had to control the inner endoscope via observations on the monitor of the outer endoscope. This is different from standard endoscopic procedures in which images are observed on the monitor of the endoscope which the operator is controlling.

In general, it is not easy for trainees to understand appropriate surgical procedures, i.e. where to cut and where to stabilize. Verbal communication during operation is important to facilitate appropriate assistance, which was not adequately utilized in the first series. These issues are to be learned through years of experience and cannot be achieved instantly.

As mentioned above, the difference between the two experiments may reveal that for these flexible endoscopes, surgical experience is an important factor, when the system is indicated for surgical procedures. The limitation of the inner endoscopes, not having CCD may have emphasized this issue. Consequently, the next system is to consist of two inner endoscopes with a CCD for each. This would allow the operators to control the inner endoscopes in such a manner as used for standard gastrointestinal endoscopic procedures.

Furthermore, we think that there should be two styles of design for future flexible endoscopic surgical systems; one with increased surgical maneuverability designed particularly for the techniques of surgeons, the other preserving flexible endoscopic maneuverability for endoscopists. Although it has not been decided yet which design is more appropriate for a future surgical system, endoscopists may be able to become accustomed to the flexible endoscopic surgical system with surgical maneuverability when the system is popularized.

In addition to the merits mentioned above, flexible endoscopic materials can theoretically be made compatible with X-ray systems such as fluoroscopes and computed tomography (CT) systems, exemplified by such procedures as X-ray guided bronchoscopy. In the future, the materials used for flexible endoscopic constructions are expected to acquire compatibility with the magnetic fields of magnetic resonance imaging (MRI) systems.

As mentioned before, limitations in visualization pose surgical problems even for experienced surgeons. This may only partially be solved by the subjective ability of surgeons to presume the identity of invisible objects using their tactile sense and their intuition. Actually, the compatibility with imaging systems was one of the important requirements for the design of the flexible endoscopic surgical system,

allowing visibility of anatomical information invisible to the surgeon's eyes.

In order to make one more step towards the future for less invasive and more effective medical treatments, we believe that future surgical systems should acquire the accessibility to narrow regions located deep inside the body together with the compatibility of imaging systems such as CT and MRI. Thus, from the flexible nature and structural characteristics of a non-jointed, smooth outer sheath, we selected the flexible endoscope as the conceptual basis of development for our system. It is the combination of these and the aforementioned aspects that allows for minimization in invasiveness, through the use of pre-existing natural structures and tracts for lesion access to deep regions, and with the presence of multiple interchangeable inner-scopes, an increase in distal tip functionality at the surgical site. Although there are several factors still to discuss and develop, the concept of the flexible endoscopic surgical system is considered an appropriate development for a future surgical robotic system with this current system being a successful step towards that furture.

Acknowledgments

This study was supported by a Grant-in-Aid for Research on Medical Devices for Analyzing, Supporting and Substituting the Function of Human Body from the Ministry of Health, Labour and Welfare.

References

1. Kobayashi T, Gotohda T, Tamakawa K, Ueda H, Kakizoe T. Magnetic anchor for more effective endoscopic mucosal resection. *Jpn J clin Oncol* 2004;34:118–23.
2. Gotoda T, Yanagisawa A, Sasako M, Ono H, Nakanishi Y, Shimoda T, et al. Incidence of lymph node metastasis from early gastric cancer: estimation with a large number of cases at two large centers. *Gastric Cancer* 2000;3:219–25.
3. Gotoda T, Kondo H, Ono H, Saito Y, Yamaguchi H, Saito D, et al. A new endoscopic mucosal resection procedure using an insulation-tipped electrosurgical knife for rectal flat lesions: report of two cases. *Gastrointest Endosc* 1999;50:560–3.
4. D'Anniballe A, Fiscon V, Trevisan P, Pozzobon M, Gianfreda V, Sovernigo G, et al. The da Vinci robot in right adrenalectomy: considerations on technique. *Surg Laparosc Endosc Percutan Tech* 2004;14:38–41.
5. Schiff J, Li PS, Goldstein M. Robotic microsurgical vasovasostomy and vasoepididymostomy: a prospective randomized study in a rat model. *J Urol* 2004;171:1720–5.
6. Ruurda JP, Broeders IA, Simmermacher RP, Borel Rinkes IH, Van Vroonhoven TJ, Theo JM. Feasibility of robot-assisted laparoscopic surgery: an evaluation of 35 robot-assisted laparoscopic cholesystectomies. *Surg Laparosc Endosc Percutan Tech* 2002;12:41–5.
7. Falk V, Diegler A, Walther T, Autschbach R, Mohr FW. Developments in robotic cardiac surgery. *Curr Opin Cardiol* 2000;15:378–87.
8. Hollands CM, Dixey LN. Applications of robotic surgery in pediatric patients. *Surg Laparosc Endosc Percutan Tech* 2002;12:71–6.

^{11}C-Acetate Positron Emission Tomography Imaging for Lung Adenocarcinoma 1 to 3 cm in Size With Ground-Glass Opacity Images on Computed Tomography

Hiroaki Nomori, MD, PhD, Noboru Kosaka, MD, PhD, Kenichi Watanabe, MD, Takashi Ohtsuka, MD, Tsuguo Naruke, MD, PhD, Toshiaki Kobayashi, MD, PhD, and Kimiichi Uno, MD, PhD

Department of Thoracic Surgery, Graduate School of Medical and Pharmaceutical Sciences, Kumamoto University; Department of Thoracic Surgery, Saiseikai Central Hospital; Development in Assistive Diagnostic Technology, National Cancer Center Hospital, and Nishidai Clinic, Tokyo, Japan

Background. Positron-emission tomography (PET) with ^{18}F-fluorodeoxy-glucose (FDG) frequently gives false-negative results for well-differentiated adenocarcinomas of the lung, especially, those with ground-glass opacity images. Recently, PET with ^{11}C-acetate (AC) has been reported to detect slow-growing tumors that have failed to be identified by FDG-PET, such as well-differentiated hepatocellular carcinomas and prostate cancers. To determine the usefulness of AC-PET in detecting well-differentiated adenocarcinomas of the lung, we performed both AC-PET and FDG-PET on pulmonary nodules with ground-glass opacity images on computed tomography (CT).

Methods. Fifty-four pulmonary nodules 1 to 3 cm in size, which showed ground-glass opacity images over their whole or peripheral area on CT, were examined by both AC-PET and FDG-PET.

Results. Thirty-seven nodules were adenocarcinoma of the lung, while 17 were inflammatory. Of the 37 adenocarcinomas, 19 (51%) were positively identified by AC-PET and 14 (38%) by FDG-PET. Of the 23 adenocarcinomas which were not identified by FDG-PET, 8 (35%) were positively identified by AC-PET; all were well-differentiated adenocarcinomas. Of the 17 inflammatory nodules, 8 were chronic and 9 were acute ones. While none of the 8 chronic inflammatory nodules were identified by either technique, 9 acute ones showed a variety of the results with AC- and FDG-PET.

Conclusions. AC-PET detected approximately one third of well-differentiated adenocarcinomas of the lung which were not identified by FDG-PET. AC-PET could be useful to diagnose pulmonary nodules with ground-glass opacity images which were not identified by FDG-PET.

(Ann Thorac Surg 2005;80:2020–5)

Recent advances in positron emission tomography (PET) with ^{18}F-fluorodeoxy-glucose (FDG) have contributed significantly to the ability to differentiate between benign and malignant pulmonary nodules. However, FDG-PET sometimes gives false-negative results, particularly for low-grade malignant tumors, such as bronchioloalveolar carcinoma and carcinoid, owing to their low glucose metabolism [1–4]. We previously reported that while FDG-PET did not produce false-negative results for squamous cell, large cell, or small cell carcinomas, 60% of well-differentiated adenocarcinomas 1 to 3 cm in size failed to be identified by FDG-PET [2]. Therefore, other PET tracers should be used for imaging suspected well-differentiated adenocarcinoma of the lung.

Radio-labeled acetate has long been used for the measuring lipid and cholesterol synthesis in biochemistry [5, 6]. Clinically, ^{11}C-acetate (AC) has been widely used as a PET tracer for evaluating myocardial oxidative metabolism [7, 8]. Recently, AC has also been reported to be a useful PET tracer in detecting slow-growing tumors which have failed to be identified by FDG-PET, such as well-differentiated hepatocellular carcinomas and prostate cancers [9, 10]. Higashi and colleagues [11] have also reported a patient with bronchioloalveolar carcinoma that was positively identified by AC-PET but not by FDG-PET. In the present study, to evaluate the effectiveness of AC-PET in detecting well-differentiated adenocarcinomas of the lung, we performed both AC-PET and FDG-PET on 54 small pulmonary nodules suspected of being adenocarcinomas based on computed tomography (CT) findings.

Material and Methods

Patients and Tumor Tissues

The pulmonary nodules of 1 to 3 cm in size, which were suspected of being well-differentiated adenocarcinoma of

Accepted for publication June 3, 2005.

Address correspondence to Dr Nomori, Department of Thoracic Surgery, Graduate School of Medical and Pharmaceutical Sciences, Kumamoto University, 1-1-1 Honjo, Kumamoto 860-8556, Japan; e-mail address: hnomori@qk9.so-net.ne.jp.

Published by Elsevier Inc

0003-4975/05/$30.00
doi:10.1016/j.athoracsur.2005.06.003

Table 1. FDG-PET and Acetate-PET Findings in Adenocarcinomas and Inflammatory Nodules

Procedures	Adenocarcinoma	Inflammation	Total
FDG-PET			
Positive	14	5	19
Negative	23	12	35
Acetate-PET			
Positive	19	5	24
Negative	18	12	30
Total	37	17	54

FDG = fluorodeoxyglucose; PET = positron emission tomography.

the lung owing to the presence of ground-glass opacity images over their whole or peripheral area on CT [12–15], were performed of both FDG-PET and AC-PET to evaluate the usefulness of AC-PET. The study was approved by the Ethical Committee of Saiseikai Central Hospital in December 2003. The reason why we excluded the nodules less than 1 cm was that the spatial resolution of the current generation of PET scanners is 0.7 to 0.8 cm, making it difficult to image pulmonary nodules of less than 1 cm [2]. Between January 2004 and April 2005, 54 pulmonary nodules with ground-glass opacity images in 50 patients were enrolled. Three patients have a few nodules, which were located in the different lobes of each other in each patient. During the same period, 85 pulmonary nodules up to 3 cm with solid images in 82 patients were examined only by FDG-PET. Of the 54 nodules, 37 were adenocarcinoma of the lung and 17 were inflammatory. The diagnosis was confirmed histologically after surgical resection in all 37 of the adenocarcinomas, 8 of the nodules with chronic inflammation, 2 with active tuberculosis, and 1 with active nonspecific inflammation. The remaining 6 nodules were clinically diagnosed as acute inflammatory nodules because of natural reduction on follow-up CT. The lung adenocarcinomas were classified as well-, moderately, and poorly differentiated. The percentage area showing ground-glass opacity on CT was graded as more than 90%, 30% to 90%, or less than 30%.

Positron Emission Tomography Scanning

Positron emission tomography scanning was performed at Nishidai Clinic, Tokyo, Japan. Patients were instructed to fast for at least 4 hours before PET scanning. After a written informed consent had been obtained, AC- and FDG-PET were performed on the same day within 2 weeks of CT scanning. The AC-PET was performed before FDG-PET. The dose of ^{11}C-AC administered was 125 μCi/kg (4.6 MBq/kg). The PET imaging was performed approximately 10 minutes after the administration of ^{11}C-AC using a PosiCam.HZL mPower scanner (Positron, Houston, Texas).

The ^{18}F-FDG was administered approximately 30 minutes after AC-PET imaging was completed, ensuring that a gap of at least 120 minutes was left between the administration of ^{11}C-AC and that of ^{18}F-FDG, namely, more than 6 decay half-lives of ^{11}C (20 minutes). The dose of ^{18}F-FDG was 125 μCi/kg (4.6 MBq/kg) for nondiabetic patients and 150 μCi/kg (5.6 MBq/kg) for diabetic patients, as reported previously [2–4]. The FDG-PET imaging was performed approximately 45 minutes after the administration of FDG.

No attenuation-corrected emission scans were initially obtained in two-dimensional, high-sensitivity mode for 4 minutes per bed position, and taken from the vertical skull through to the mid thighs. Immediately thereafter, a two-bed–position, attenuation-corrected examination was performed, with 6 minutes for the emission sequence and 6 minutes for the transmission sequence at each bed position. The images were reconstructed by the emission scans and the preinjection transmission scans in a 128 × 128 matrix by using ordered subset expectation maximization corresponding to a pixel size of 4 × 4 mm, with section spacing of 2.56 mm.

Positron Emission Tomography Data Analysis

Images were reviewed by two observers (N.K. and K.U.) who were unaware of the patients' clinical details. A consensus was reached if there was any difference of opinion. PET images were evaluated by visual assessment, namely, lesions showing similar or greater AC or FDG uptake than the mediastinal blood pool were diagnosed as positive for tumor. The AC and FDG uptakes of the positive nodules were measured on the basis of the contrast ratio, as reported previously [2–4]. Briefly, regions of interest were chosen in the nodules and contralateral lung. The highest standard uptake value in the tumor regions of interest (T) and the contralateral normal lung regions of interest (N) were then measured and the contrast ratio was calculated as $(T - N)/(T + N)$ in each nodule as an index of AC and FDG uptake.

Evaluation by Receiver Operating Characteristics Curve

Usefulness of detecting well-differentiated adenocarcinoma by FDG- and AC-PET was evaluated by receiver operating characteristics (ROC) curves. The contrast ratio values of 27 well-differentiated adenocarcinomas and 27 other lesions (10 moderately or poorly differentiated adenocarcinomas and 17 inflammatory nodules) of FDG-PET and AC-PET were compared on ROC curve by using SPSS software (SPSS, Chicago, Illinois).

Statistical Analysis

Positive PET findings with malignancy and benign nodules were defined as true positive (TP) and false positive

Table 2. Summary of Results of FDG-PET and Acetate-PET

Variables	FDG-PET	Acetate-PET
Sensitivity	0.38	0.51
Specificity	0.71	0.71
Positive predictive value	0.74	0.79
Negative predictive value	0.34	0.40
Accuracy	0.48	0.57

FDG = fluorodeoxyglucose; PET = positron emission tomography.

Ann Thorac Surg
2005;80:2020–5

Table 3. Correlation Between Histologic Grade of Differentiation of Adenocarcinomas and PET Findings

PET Imaging Findings	Histologic Differentiation			Total
	WD	MD	PD	
Acetate positive, FDG positive	5	5	1	11
Acetate positive, FDG negative	8	0	0	8
Acetate negative, FDG positive	0	3	0	3
Acetate negative, FDG negative	14	1	0	15
Total	27	9	1	37

FDG = fluorodeoxyglucose; MD = moderately differentiated; PD = poorly differentiated; PET = positron emission tomography; WD = well differentiated.

(FP), respectively. Negative PET findings with malignancy and benign nodules defined as false negative (FN) and true negative (TN), respectively. The diagnostic values of PET scanning were assessed by calculating sensitivity and specificity. Sensitivity was calculated as TP/TP + FN, specificity as TN/TN + FP, positive predictive value as TP/TP + FP, negative predictive value as TN/FN + TN, and accuracy as TP + TN/total. All data were analyzed for significance by using the two-tailed Student t test. Values of p less than 0.05 were accepted as significance. All values in the text and tables are given as mean ± SD.

Results

Table 1 shows the PET findings of adenocarcinomas and inflammatory nodules. Mean sizes were 2.1 ± 0.7 cm for the 37 adenocarcinomas and 1.7 ± 0.8 cm for the 17 inflammatory nodules; this difference was not significant. Of the 37 adenocarcinomas, 19 were positively identified by AC-PET and 14 by FDG-PET. The sensitivity, specificity, positive predictive value, negative predictive value, and accuracy were not significant different between the FDG-PET and AC-PET (Table 2). Eleven adenocarcinomas were positively identified by both AC- and FDG-PET, 8 were positively identified by AC-PET but not by FDG-PET, 3 were positively identified by FDG-PET but not by AC-PET, and the remaining 15 failed to be identified by either technique (Table 3). Of the 17 inflammatory nodules, 3 were positively identified by both AC-PET and FDG-PET, 2 were positively identified by AC-PET but not by FDG-PET, 2 were positively identified by FDG-PET but not by AC-PET, and the remaining 10 were negative by either technique (Table 4).

Table 4. FDG-PET and Acetate-PET Findings in Inflammatory Nodules

PET Imaging Findings	Chronic Inflammation	Acute Inflammation	Total
Acetate positive, FDG positive	0	3	3
Acetate positive, FDG negative	0	2	2
Acetate negative, FDG positive	0	2	2
Acetate negative, FDG negative	8	2	10
Total	8	9	17

FDG = fluorodeoxyglucose; PET = positron emission tomography.

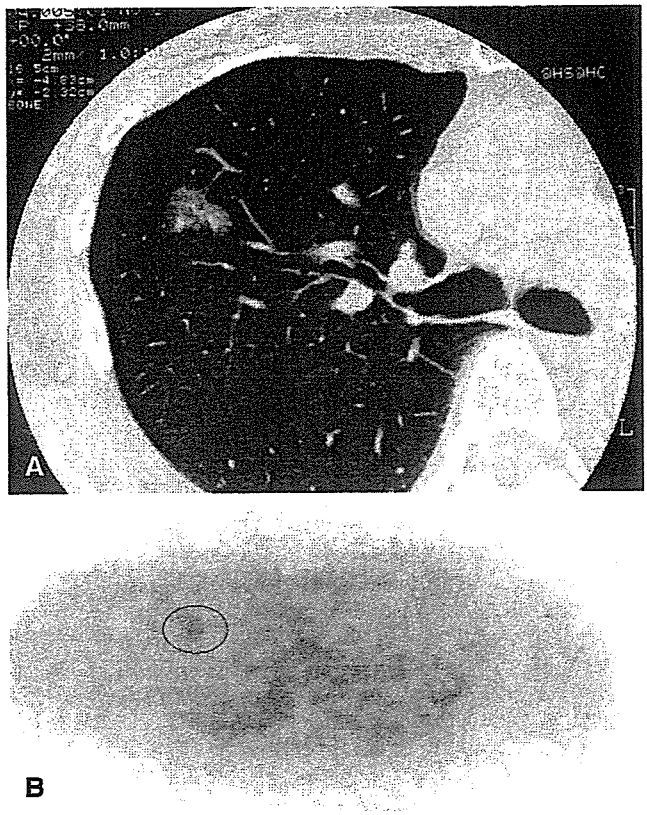

Fig 1. (A) Computed tomography findings of well-differentiated adenocarcinoma with ground-glass opacity findings. (B) Acetate-positron emission tomography showed positive at the tumor (encircled).

Table 3 also shows the correlation between the histologic grade of differentiation and the PET findings in the 37 adenocarcinomas. The histologic grades were well differentiated in 27 adenocarcinomas, moderately differentiated in 9, and poorly differentiated in 1. Of the 23 adenocarcinomas which failed to be identified by FDG-PET, 8 (36%) were positively identified by AC-PET, all of which were well-differentiated ones (Fig 1), whereas none of moderately or poorly differentiated adenocarcinomas were positive with AC-PET and negative with FDG-PET. Well-differentiated adenocarcinomas were more frequently positive with AC-PET and negative with FDG-PET than moderately or poorly differentiated adenocarcinomas (p = 0.051). Of the 15 adenocarcinomas which failed to be identified by either technique, 14 (93%) were well-differentiated ones and the remaining 1 (7%) was moderately differentiated. Well-differentiated ade-

Table 5. Correlation Between Percent of GGO Area and Histologic Grade of Differentiation of Adenocarcinomas

	Histologic Differentiation			
Percent of GGO Area	WD	MD	PD	Total
≥90%	19[a]	1	0	20
30%–90%	5	0	0	5
<30%	3	8	1	12
Total	27	9	1	37

[a] Well-differentiated adenocarcinoma showed more than 90% of GGO area more frequently than moderately or poorly differentiated ($p < 0.01$).

GGO = ground-glass opacity; MD = moderately differentiated; PD = poorly differentiated; WD = well-differentiated.

nocarcinomas were more frequently negative with both AC-PET and FDG-PET than moderately or poorly differentiated adenocarcinomas ($p = 0.03$).

Both AC and FDG uptake of these adenocarcinomas were usually weak by visual assessment. In the 19 adenocarcinomas detected by AC-PET, the mean values of contrast ratio and standard uptake value were 0.3 ± 0.1 (range, 0.25 to 0.42) and 2.3 ± 0.7 (range, 1.1 to 3.4), respectively. In the 13 adenocarcinomas detected by FDG-PET, the mean values of contrast ratio and standard uptake value was 0.4 ± 0.2 (range, 0.25 to 0.8) and 3.2 ± 1.8 (range, 1.0 to 7.4), respectively.

Table 4 shows the FDG- and AC-PET findings in the 17 inflammatory nodules. While none of the 8 nodules with chronic inflammation were detected by either AC- or FDG-PET, 9 nodules with acute inflammation showed a variety of the results.

Table 5 shows the correlation between the percentage area of ground-glass opacity and the histologic grade of differentiation in the 37 adenocarcinomas. Ground-glass opacity was apparent over more than 90% of the tumor area in 20 adenocarcinomas, 30% to 90% in 5, and less than 30% in the remaining 12. Well-differentiated adenocarcinomas showed more than 90% of ground-glass opacity area more frequently than moderately or poorly differentiated ones ($p < 0.01$).

Figure 2 shows the ROC curves of FDG- and AC-PET for detecting 27 well-differentiated adenocarcinoma in the 54 nodules with ground-glass opacity images. The ROC curve of AC-PET was superior to that of FDG-PET. The areas under the curve were 0.573 in AC-PET and 0.318 in FDG-PET. The 95% confidential limits showed little overlap between the AC-PET (range, 0.414 to 0.733) and FDG-PET (range, 0.174 to 0.461).

The tumor size did not show any correlation not only with contrast ratio values and standard uptake value of FDG-PET ($r = 0.31$ and $r = 0.38$, respectively) but also with contrast ratio values and standard uptake value of AC-PET ($r = 0.1$ and $r = 0.08$, respectively).

Comment

While a criterion for diagnosing pulmonary malignancy with FDG-PET has frequently used the standard uptake value with a cut-off value of 2.5 [16], it has been reported that several factors can affect the standard uptake value, such as the body size [17], blood glucose concentration [18], time after injection [19], and lesion size [20]. Actually, the mean standard uptake value of malignant pulmonary nodules has been reported to be various, ranging from 5.5 to 10.1 [21–24]. We previously compared the results of standard uptake value, contrast ratio with contralateral lung, and contrast ratio with cerebellum for diagnosing pulmonary nodules with faintly positive FDG uptake by visual estimation, and reported the cut-off value of 0.4 by the contrast ratio with contralateral lung to show the highest sensitivity, while the standard uptake value of 2.5 showing the sensitivity of 0 [25]. We therefore used the contrast ratio with contralateral lung in the present study. Both AC and FDG uptake in the present adenocarcinomas were usually weak. The mean contrast ratio values of AC and FDG uptake of the positive adenocarcinomas in the present study were 0.3 ± 0.1 and 0.4 ± 0.2, respectively, both of which were near the cut-off value for diagnosing lung cancers. It could be due to that most of adenocarcinomas in the present study were well-differentiated ones, which were known to show weak or negative PET imaging frequently [1–4].

Well-differentiated adenocarcinomas of the lung have been reported to show a high false-negative identification rate on FDG-PET because of their low glucose metabolism and low tumor cell density [1–4]. These observations were confirmed by the present study in which 22 of the 27 well-differentiated adenocarcinomas (81%) failed to be detected by FDG-PET (as shown in Table 3). While ^{11}C-AC has been reported to be a useful PET tracer for slow-growing tumors, such as well-

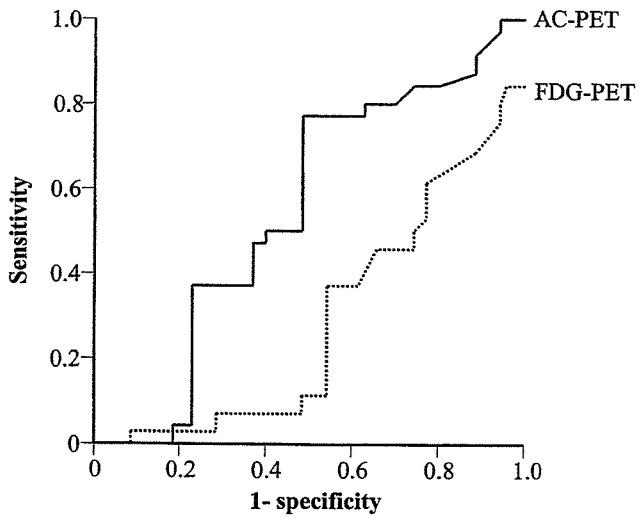

Fig 2. The receiver operating characteristic curve of ^{11}C-acetate positron emission tomography (AC-PET; solid line) *and ^{18}F-fluorodeoxy-glucose PET* (FDG-PET; dotted line) *for detecting 27 well-differentiated adenocarcinoma in the 54 nodules with ground-glass opacity images. The areas under the curve were 0.573 in AC-PET and 0.318 in FDG-PET. The 95% confidence limits were from 0.414 to 0.733 in AC-PET and from 0.174 to 0.461 in FDG-PET.*

differentiated hepatocellular carcinomas and prostate cancers [9, 10], the present study showed that there was no significant difference in sensitivity between AC-PET and FDG-PET with respect to adenocarcinomas of the lung. However, of the 23 adenocarcinomas not identified by FDG-PET, 8 (35%) were positively identified by AC-PET; all of these were well-differentiated adenocarcinomas. Therefore, AC-PET was able to detect approximately one third of well-differentiated adenocarcinomas that were not detected by FDG-PET.

Ho and Yeung [9] reported that while well-differentiated hepatocellular carcinomas had a high AC uptake and a low FDG uptake, poorly differentiated ones had a low AC uptake and a high FDG uptake. Thus, hepatocellular carcinomas could be detected with 100% sensitivity by using both AC-PET and FDG-PET [9]. In contrast, Oyama and colleagues [10] reported that all 22 of their patients' prostate cancers were positively identified by AC-PET. However, the present study showed that 15 of the 37 lung adenocarcinomas (41%) could not be detected by either AC- or FDG-PET, and 14 of these 15 (93%) were well-differentiated adenocarcinomas. There are several reasons why well-differentiated adenocarcinomas of the lung may frequently go undetected by both AC-PET and FDG-PET. Firstly, well-differentiated lung adenocarcinomas may accumulate AC and FDG to only a limited extent due to lower metabolism of these substances compared with hepatocellular carcinomas and prostate cancers. Secondly, because well-differentiated adenocarcinomas frequently show ground-glass opacity images over a large area (as shown in Table 5), the density of the tumor cells is low compared with moderately or poorly differentiated ones, and that could be false-negative results of PET imaging, regardless of the degree of tracer uptake by the tumor cells. Thirdly, because all the adenocarcinomas in the present study were less than 3 cm in size, their AC or FDG uptake may have been below the limit of detection compared with larger ones.

The tracer ^{11}C-acetate has been widely used as a PET tracer for the evaluation of myocardial oxidative mechanism [7, 8]. The mechanism underlying AC uptake in tumor cells, although as yet unknown, is thought to be different from that involved in myocardial uptake. In an in vitro study using several cancer cell lines, Yoshimoto and colleagues [25] suggested that AC is preferentially metabolized to membrane lipids in tumor cells and that AC uptake by tumor cells reflects their growth activity as measured by enhanced membrane synthesis. On the other hand, Ho and Yeung [9] reported that the AC uptake of hepatocellular carcinomas showed negative correlation with their malignant potential. In the present study, while some of the well-differentiated adenocarcinomas were positively identified by AC-PET but not by FDG-PET, some of the well-, moderately, and poorly differentiated adenocarcinomas were positively identified by both technique. Based on our present data, we hypothesize the following: (1) Whereas FDG may be accumulated by aggressive lung cancer cells [26, 27], AC might be accumulated by slow-growing ones, as in the case with hepatocellular carcinomas and prostate cancers [9, 10]. (2) Whereas most lung cancers can accumulate both AC and FDG because of containing tumor cells having different growth activity, some well-differentiated adenocarcinomas, which only contain less aggressive tumor cells, may be able to accumulate only AC.

Both chronic and acute inflammatory pulmonary nodules are well known to show ground-glass opacity images on occasions. In the present study, while all of the chronic inflammatory nodules were negative by both AC-PET and FDG-PET, the acute ones showed a variety of the results. That could be because the acute inflammatory nodules have a variety of percentages of inflammatory cells having different grades of metabolic activity, such as leukocytes, lymphocytes, and macrophages, according to the phase of inflammation.

Positron emission tomography with AC could be useful for some of pulmonary nodules with ground-glass opacity images that could not be identified by FDG-PET. In the present study, most of the nodules studied were well-differentiated adenocarcinomas because the nodules were selected on the basis of the presence of ground-glass opacity images. Therefore, AC-PET needs to be studied in other histologic types of lung cancer to clarify its usefulness in detecting lung cancers in general.

This work was supported in part by a Grant-in-Aid from the Ministry of Health, Labor and Welfare of Japan.

References

1. Higashi K, Ueda Y, Seki H, et al. Fluorine-18-FDG PET imaging is negative in bronchioloalveolar carcinoma. J Nucl Med 1998;39:1016–20.
2. Nomori H, Watanabe K, Ohtsuka T, Naruke T, Suemasu K, Uno K. Evaluation of F-18 fluorodeoxyglucose (FDG) PET scanning for pulmonary nodules less than 3 cm in diameter, with special reference to the CT images. Lung Cancer 2004;45:19–27.
3. Nomori H, Watanabe K, Ohtsuka T, et al. Fluorine 18-tagged fluorodeoxyglucose positron emission tomographic scanning to predict lymph node metastasis, invasiveness, or both, in clinical T1N0M0 lung adenocarcinoma. J Thorac Cardiovasc Surg 2004;128:396–401.
4. Nomori H, Watanabe K, Ohtsuka T, Naruke T, Suemasu K, Uno K. Visual and semiquantitative analyses from F-18 fluorodeoxyglucose (FDG) PET scanning in pulmonary nodules 1 to 3 cm in size. Ann Thorac Surg 2005;79:984–8.
5. Howard BV. Acetate as a carbon source for lipid synthesis in cultured cells. Biochim Biophys Acta 1977;488:145–51.
6. Long VJW. Incorporation of 1-11C-acetate into the lipids of isolated epidermal cells. Br J Dermatol 1976;94:243–52.
7. Brown M, Marshall DR, Sobel BE, Bergmann SR. Delineation of myocardial oxygen utilization with carbon-11-labeled acetate. Circulation 1987;76:687–96.
8. Lear JL. Relationship between myocardial clearance rates of carbon-11-acetate-deribed radiolabel and oxidative metabolism: physiologic basis and clinical significance. J Nucl Med 1991;32:1957–60.
9. Ho C, Yeung DW. C-11 acetate PET imaging in hepatocellular carcinoma and other liver masses. J Nucl Med 2003;44:213–21.
10. Oyama N, Akino H, Kanamaru H, et al. 11C-acetate PET imaging of prostate cancer. J Nucl Med 2002;43:181–6.

11. Higashi K, Ueda Y, Matsunari I, et al. 11C-acetate PET imaging of lung cancer: comparison with 18F-FDG and 99mTc-MIBI SPET. Eur J Nucl Med Mol Imaging 2004; 31:13–21.
12. Aoki T, Nakata H, Watanabe H, et al. Evolution of peripheral lung adenocarcinomas: CT findings correlated with histology and tumor doubling time. Am J Roentgenol 2000;174: 763–8.
13. Nakata M, Saeki H, Takata I, et al. Focal ground-glass opacity detected by low-dose helical CT. Chest 2002;121: 1464–7.
14. Nomori H, Ohtsuka T, Naruke T, Suemasu K. Differentiating between atypical adenomatous hyperplasia and bronchioloalveolar carcinoma using the computed tomography number histogram. Ann Thorac Surg 2003;76:867–71.
15. Nomori H, Ohtsuka T, Naruke T, Suemasu K. Histogram analysis of computed tomography numbers of clinical T1N0M0 lung adenocarcinoma, with special reference to lymph node metastasis and tumor invasiveness. J Thorac Cardiovasc Surg 2003;126:1584–9.
16. Langen KJ, Braun U, Rota Kops E, et al. The influence of plasma glucose levels of fluorine-18-fluorodeoxyglucose uptake in bronchial carcinomas. J Nucl Med 1993;34:355–9.
17. Kim CK, Gupta NC, Chandramouli B, Alavi A. Standarized uptake values of FDG: body surface area correction is preferable to body weight correction. J Nucl Med 1994;35: 164–7.
18. Lindholm P, Minn H, Leskinen-Kallio S, Bergman J, Ruotsalainen U, Joensuu H. Influence of the blood glucose concentration on FDG uptake in cancer—a PET study. J Nucl Med 1993;34:1–6.
19. Hamberg LM, Hunter GI, Alpert NM, Choi NC, Babich JW, Fischman AJ. The dose uptake ratio as an index of glucose metabolixm: useful parameter or oversimplification? J Nucl Med 1994;35:1308–12.
20. Menda Y, Bushnell DL, Madsen MT, McLaughlin K, Kahn D, Kernstine KH. Evaluation of various corrections to the standardized uptake value for diagnosis of pulmonary malignancy. Nucl Med Commun 2001;22:1077–81.
21. Dewan NA, Gupta NC, Redepenning LS, et al. Diagnostic efficacy of PET-FDG imaging in solitary pulmonary nodules. Chest 1993;104:997–1002.
22. Gupta NC, Maloof J, Gunel E. Probability of malignancy in solitary pulmonary nodules using fluorine-18-FDG and PET. J Nucl Med 1996;37:943–8.
23. Imdahl A, Jenkner S, Brink I, et al. Validation of FDG positron emission tomography for differentiation of unknown pulmonary lesions. Eur J Cardiothorac Surg 2001;20: 324–9.
24. Lowe VJ, Fletcher JW, Gobar L, et al. Prospective investigation of positron emission tomography in lung nodules. J Clin Oncol 1998;16:1075–84.
25. Yoshimoto M, Waki A, Yonekura Y, et al. Characterization of acetate metabolism in tumor cells in relation to cell proliferation: acetate metabolism in tumor cells. Nucl Med Biol 2001;28:117–22.
26. Higashi K, Ueda Y, Yagishita M, et al. FDG PET measurement of the proliferative potential on non-small cell lung cancer. J Nucl Med 2000;41:85–92.
27. Vesselle H, Schmidt RA, Pugsley JM, et al. Lung cancer proliferation correlates with [F-18] fluorodeoxyglucose uptake by positron emission tomography. Clin Cancer Res 2000;6:3837–44.